

Storm Surge Forecast System for Floodfighting Warning

by

Masaya Fukuhama¹ and Fuminori Kato²

ABSTRACT

This paper presents current developments in a real-time forecast system for wave runup to ensure proper floodfighting warning in coastal areas. The system consists of a typhoon model, storm surge model, wave models, and a wave runup model. A wave model for shallow water was developed through numerical tests on precision and time of hindcasting. The results of the tests show that an improved WAM that considers wave breaking and tides can forecast waves in inner bays with good precision in real time.

KEYWORDS: Floodfighting Warning, Real-time Forecast, Storm Surge, Wave Runup

1. INTRODUCTION

Japan's Flood Fighting Law stipulates that prefectural governors shall issue a floodfighting warning of storm surges in coast areas previously recognized as being at high risk. Floodfighting warnings are transmitted to the administrators (mayors, etc.) of floodfighting activities such as patrolling coasts and closing water gates. However, forecasts of storm surges and high waves before a typhoon approach are not sufficient information for issuing a floodfighting warning because the forecasts do not indicate if the wave runup exceeds the coastal dikes. Also, wave forecasts are not very precise, particularly near the coasts because wave models do not consider wave transformation in shallow water, such as shoaling and refraction. Therefore, we are developing a wave runup forecast system to ensure proper floodfighting warnings.

2. WAVE RUNUP FORECAST SYSTEM

As shown in Fig. 1, the system forecasts wave runup on each coast every hour for 24 hours

based on storm surges and high waves estimated by the Japan Meteorological Agency (JMA). Wave runup is calculated by the Improved Imaginative Slope Method [1], a simple method often used for designing shore protection facilities in Japan. The forecasted wave runup is edited in graphs and tables, and delivered via Intranet and Internet to regional bureaus of MLIT and prefectures. The graphs that show predicted wave runup and height of coastal dikes is important information for deciding when and on which coasts a floodfighting warning is issued. The system can predict the worst-case scenario because wave runup is forecasted for five typhoon courses based on the probability circle forecasted for the typhoon. The predicted wave runup is updated every six hours.

3. DEVELOPMENT OF WAVE FORECAST MODEL

JMA forecasts waves near Japan using the Regional Wave Model, in which ocean waves forecasted by the Global Wave Model are used as boundary conditions. As of March 2007, the grid size of the Regional Wave Model is 6 min in polar coordinates (about 10 km long). The model does not consider wave transformation in shallow water, such as shoaling and refraction. Therefore, reproducibility of bathymetry and wave transformation is limited for inner seas with complicated bathymetry.

In this study, we examined wave models to precisely forecast waves in inner seas by using forecasts of the Regional Wave Model as boundary conditions, considering bathymetry and wave transformation in shallow water.

¹ Head, Coast Division, River Department, National Institute for Land and Infrastructure Management, Ministry of Land, Infrastructure and Transport (MLIT), Asahi 1, Tsukuba-shi, Ibaraki-ken 305-0804, Japan

² Senior Researcher, Coast Division, NILIM

3.1 Review of Wave Forecasting Model

3.1.1 Comparison of Wave Forecasting Models
WAM (WAve Model) and SWAN (Simulating WAves Nearshore) are major wave hindcasting models that can be applied for shallow water. WAM is widely used for estimating ocean waves, and its applicability to hindcasting in inner seas has been reviewed in recent years [2-5]. SWAN is a third-generation wave model the same as WAM and can also consider wave breaking. Wave transformation models, which consider not winds but reflection and wave breaking etc., are often used for designing shore protection facilities. They do not consider generation and growth of waves, but need only a short time to calculate nearshore waves.

In this study, wave models were examined for major typhoons between 1997 and 2004, in Ise Bay, Harima Sea and Ariake Sea as shown in Figs. 2-4. The computation areas are divided as shown in Table 1. Preciseness and time of hindcasting were compared between cases in which WAM (Cycle 4), SWAN (40.41), and a wave transformation model based on energy balance equation were set in each computation area as shown in Table 2. Target fields of this study are the Middle Area and the Narrow Area. WAM was used for hindcasting waves in the Wide Areas covered by JMA's Regional Wave Model forecasts. In connecting Wide Area 3 to Wide Area 2, the number of angular components was increased with expansion of frequency band to higher frequency by spline interpolation following the rule "f to the minus five". In Cases 1-4, waves in the Middle Area were calculated on grids about 1.7 km wide, using the waves in Wide Area 3 as boundary conditions, and then were used as boundary conditions for wave calculation in the Narrow Area. In Case 5, waves in the Narrow Area were calculated using the wave transformation model (10 angular components) and the waves in Wide Area 3 as boundary conditions, without wave calculation in the Middle Area. The size of calculation grids in the Narrow Area was about 0.4 km for WAM and SWAN, and 50 m for the wave transformation model because of its small calculation model amount.

Calculation was conducted using a personal computer with a Pentium IV (3.6 GHz) processor. Bathymetry data from the Central Disaster Prevention Council was used for Ise Bay and Harima Sea. As for Ariake Sea, bathymetry data was prepared based on JTOPO30 (Japan Hydrographic Association).

A gradient wind model (Cardone-Myers Hybrid Model [6]) was used to hindcast ocean winds. As for winds on inner seas, the most precise hindcast was selected for each typhoon among JMA's grid-point value (RSM), mesoscale meteorological model (ANEMOS, developed by the Japan Weather Association), and a gradient wind model (Cardone-Myers Hybrid Model [6] + MASCON Model [7]), as shown in Table 3. Note that wind speeds estimated as above were divided by the regression coefficients of those at Hamada (Ise Bay), Eigashima (Harima Sea), and Ariake Tower (Ariake Sea).

3.1.2 Results

Waves are observed at Hamada, Eigashima, and Ariake Tower. The correlation coefficients (R), root mean square of errors (E), regression equations (A : regression coefficients, y : estimated value, x : observed value), and time to calculate waves in the Harima Sea are shown in Table 4. The correlation coefficients of wave heights were higher than those of wave periods in all cases, and the difference between cases was small. The root mean square of errors was less than 0.6 m for wave heights, but was relative large for wave periods in Cases 2 and 4 in which SWAN was used. The time to calculate waves in Case 1 was 14 min for the Middle Area and 53 min for the Narrow Area, and shortest among all cases. In Case 1, the regression coefficients of wave periods were almost 1, and those of wave heights were larger than 1, which means that the model did not underestimate on the average. As shown in Fig. 4, the time series of hindcasted waves also agreed with observed waves.

For Case 1 which was shortest in calculation time, omitting non-linear wave-wave interaction in shallow water and widening calculation grids

were examined to further reduce the calculation time. Non-linear wave-wave interaction is the energy transfer between frequency components. It is important for growth and dissipation of waves but not very effective in inner seas. The results of wave hindcast without the effects of non-linear wave-wave interaction showed that estimated wave heights are almost the same as those with the effects as shown in Fig. 5, and that the calculation time was reduced by 30%. On the other hand, wave heights and wave periods hindcasted in the Middle Area almost agreed with those in the Narrow Area.

As mentioned above, WAM with 1.7-km grids can forecast waves in inner seas in a short time with good precision. Therefore, we decided to develop a real-time wave forecast system based on WAM with 1.7-km grids.

3.2 Improvement of Wave Forecasting Model

3.2.1 Model Improvement

WAM does not consider the effects of wave breaking, although water depth is relatively small in inner seas. Besides this, tides are so large in inner seas that time variation of water depth may influence waves. To consider wave breaking and tides in wave forecasts, we combined WAM with the bore model [8] and the ocean tide model (NAO.99b) [9]. The bore model used for SWAN is a method of calculating energy dissipation based on the similarity between breaking wave and bores [2].

Table 5 shows the typhoons for which waves were hindcasted by the improved models. The computation area and the number of frequency components are the same in Table 1, but RSM winds adjusted by observed wind speeds were used in Wide Area 3 and the Middle Area.

3.2.2 Review of Improved Model

As shown in Tables 6 and 7, the effects of the model improvement were very small at Hamada (Ise Bay), but were obvious in the regression coefficients and root mean square of errors at Eigashima (Harima Sea) and Ariake Tower (Ariake Sea). For example, considering wave breaking improved hindcast precision at Ariake

Tower near the peak of wave height, as shown in Fig. 6. The effects of wave breaking were clear at Eigashima and Ariake Tower because the water depth was smaller than Hamada (20 m deep). Also, considering wave breaking and tides increased the calculation time by only 10%.

4. CONCLUSIONS

An improved WAM that considers wave breaking and tides can forecast waves in inner seas with good precision in real time. Information for proper floodfighting warning can be supplied by combining this system with the forecast system for wave runup at each coast.

This system will be operated in Tokyo Bay, Ise Bay, Osaka Bay and Harima Sea, and the Ariake Sea. Test operation for one typhoon course will start in August 2007. After solving operating problems, we will begin full-scale operation for five typhoon courses in August 2008.

ACKNOWLEDGMENTS

This study was conducted through discussion within a working group formed by the NILIM, Port and Airport Research Institute (PARI), and Meteorological Research Institute (MRI), in cooperation with the River Bureau and Port Bureau of the Ministry of Land, Infrastructure and Transport, and the Japan Meteorological Agency. Source codes of WAM improved by PARI were used in this study. Examination and improvement of wave hindcasting models were conducted with the Japan Weather Association. We express our appreciation for the bathymetry data on Ise Bay and the Harima Sea provided by the Cabinet Office of Japanese Government.

5. REFERENCES

1. Nakamura, M., Sasaki, Y., and Yamada, J.: Wave Runup on Compound Slopes, *Proceedings of 19th Japanese Conference on Coastal Engineering*, JSCE, 1972. (in Japanese)

2. Kawaguchi, K., Sugimoto, A., and Hashimoto, N.: Application of Third Generation Wave Models Coupled with Mesoscale Meteorological Models for Tokyo Bay, *Technical Note of The Port and Airport Research Institute*, No.1061, 2003. (in Japanese)
3. Hashimoto, N. and Kawaguchi, K.: Recent Progress in Wave Hindcasting Models and Their Applications, *Journal of Civil Engineering in the Ocean*, JSCE, Vol.19, 2003. (in Japanese)
4. Hashimoto, N., Matsumoto, H., Kawaguchi, K., Matsufuji, E., and Matsuura, K.: Development of Wave Hindcasting Database for Seto Inland Sea by Using Mesoscale Meteorological Model and Third Generation Wave Model, *Journal of Civil Engineering in the Ocean*, JSCE, 2004. (in Japanese)
5. Hashimoto, N., Kawaguchi, K., Ikegami, M., and Suzuyama K.: Study on Applicability of Third Generation Wave Model WAM for Tokyo Bay, *Journal of Civil Engineering in the Ocean*, JSCE, 2004. (in Japanese)
6. Okada, K., Hayashi, K., and Isozaki, I.: A Development of A Sea Surface Wind Estimation Method in Inland Sea, *Oceanography in Japan*, Vol.4, No.2, 1995. (in Japanese)
7. Sherman, C., A.: A Mass-consistent Model for Wind Fields over Complex Terrain, *Journal of Applied Meteorology*, Vol.17, 1978.
8. Battjes, J. A. and Janssen, J. P. F. M.: Energy Loss and Set-up due to Breaking of Random Waves, *Proceedings of the 16th International Conference on Coastal Engineering*, ASCE, 1978.
9. Matsumoto, K., Takanezawa, T. and Ooe, M.: Ocean Tide Models Developed by Assimilating TOPEX/ POSEIDON Altimeter Data into Hydrodynamical Models: A Global Model and A Regional Model around Japan, *Journal of Oceanography*, Vol. 56, 2000.

Table 1 Computation Areas

	Wide Area 1	Wide Area 2		Wide Area 3	Middle Area	Narrow Area			
Computation Area	N 15.0 - 50.0 E 120.0 - 155.0	N 30.0 - 35.5 E 128.0 - 140.0	Ise Bay	N 34.0 - 35.25 E 136.5 - 137.75	N 34.4 - 35.1 E 136.5 - 137.4	N 34.55 - 34.7 E 136.5 - 136.8			
			Harima Sea	N 33.5 - 35.0 E 134.0 - 135.5	N 34.1 - 34.8 E 134.1 - 135.5	N 34.6 - 34.8 E 134.7 - 135.05			
			Ariake Sea	N 32.0 - 33.5 E 129.25 - 130.75	N 32.45 - 33.25 E 130.05 - 130.75	N 33.05 - 33.2 E 130.1 - 130.45			
Number of Grids	71×71	49×23	Ise Bay	26×26	55×43	73×37			
			Harima Sea	31×31	85×43	85×49			
			Ariake Sea	31×31	43×49	73×37			
Grid Size	30 minutes (app. 50 km)	15 minutes (app. 25 km)	3 minutes (app. 5 km)	1 minute (app. 1.7 km)	0.25 minutes (app. 0.4 km)				
Number of Frequent Components	25 components			35 components					
	$f(1) \times 1.10^{(i-1)}$ ($f(1) = 0.04177248$)								
Period Components	2.4 to 24 seconds		0.9 - 24 seconds						
Number of Direction Components	16 components		36 components						
Wind Data	Gradient wind model		RSM, ANEMOS, gradient wind model						

Table 2 Case Setup

Case	Middle Area	Narrow Area
1	WAM	WAM
2	WAM	SWAN
3	WAM	Wave transformation model
4	SWAN	SWAN
5	-	Wave transformation model

Table 3 Wind Models for Wave Hindcast

Ise Bay		Harima Sea		Ariake Sea	
T9807	RSM	T9708	ANEMOS	T9711	Gradient wind model
T9810	RSM	T9805	RSM	T9918	ANEMOS
T0111	RSM	T9807	RSM	T0014	ANEMOS
T0310	ANEMOS	T9810	ANEMOS	T0205	RSM
T0406	RSM	T9918	ANEMOS	T0215	Gradient wind model
		T0310	ANEMOS	T0306	ANEMOS
		T0416	RSM	T0314	RSM
		T0418	RSM	T0418	ANEMOS

Table 4 Hindcast Preciseness and Calculation Time for Harima Sea

	Hamada		Eigashima		Ariake Tower		Calculation time for 24-hours wave		
	wave height	wave period	wave height	wave period	wave height	wave period	Wide Areas	Middle Area	Narrow Area
Case 1 (WAM-WAM)	R=0.81	R=0.55	R=0.91	R=0.73	R=0.86	R=0.42	1.5 minutes	14 minutes	53 minutes
	E=0.58m	E=1.49s	E=0.34m	E=1.07s	E=0.43m	E=1.26s			
	y=1.26x	y=1.09x	y=1.08x	y=1.05x	y=1.42x	y=0.99x			
Case 2 (WAM-SWAN)	R=0.81	R=0.40	R=0.85	R=0.64	R=0.85	R=0.40	1.5 minutes	14 minutes	232 minutes
	E=0.51m	E=2.58s	E=0.40m	E=1.83s	E=0.34m	E=1.82s			
	y=1.21x	y=0.48x	y=0.96x	y=0.54x	y=1.19x	y=0.50x			
Case 3 (WAM-WTM)	R=0.74	R=0.56	R=0.92	R=0.86	R=0.88	R=0.56	1.5 minutes	14 minutes	92 minutes
	E=0.55m	E=1.23s	E=0.31m	E=0.96s	E=0.48m	E=0.96s			
	y=1.11x	y=1.02x	y=0.98x	y=0.86x	y=1.48x	y=0.90x			
Case 4 (SWAN-SWAN)	R=0.81	R=0.48	R=0.97	R=0.91	R=0.95	R=0.85	1.5 minutes	113 minutes	232 minutes
	E=0.43m	E=2.83s	E=0.40m	E=2.21s	E=0.32m	E=1.61s			
	y=1.04x	y=0.44x	y=0.84x	y=0.53x	y=0.80x	y=0.52x			
Case 5 (only WTM)	R=0.73	R=0.57	R=0.92	R=0.80	R=0.87	R=0.56	1.5 minutes	-	92 minutes
	E=0.55m	E=1.34s	E=0.32m	E=0.92s	E=0.44m	E=0.96s			
	y=1.08x	y=1.06x	y=1.02x	y=0.88x	y=1.39x	y=0.88x			

R: correlation coefficients, E: root-mean-square of error, y=Ax: regression equation
WTM: wave transformation model

Table 5 Typhoons for Model Examination

Sea	Typhoon	Maximum of significant wave height (m)	Storm period
Ise Bay	T9807	3.84	20-22 Sep. 1998
	T9810	3.08	16-18 Oct. 1998
	T9805	2.78	14-16 Sep. 1998
Harima Sea	T0416	3.94	27-31 Aug. 2004
	T9810	2.85	16-18 Oct. 1998
	T0418	2.62	4-8 Sep. 2004
Ariake Sea	T0418	2.85	4-8 Sep. 2004
	T0306	2.42	16-20 Jun. 2003
	T0415	2.08	17-19 Aug. 2004
	T0314	1.84	10-13 Sep. 2003

Table 6 Correlation between Estimated Wave Height and Observed Wave Height

Sea	Model	Regression coefficient	Correlation coefficient	Root mean square of error (m)
Ise Bay	original	1.17	0.82	0.47
	+ wave breaking	1.16	0.82	0.46
	+ tides	1.18	0.82	0.48
	+ wave breaking and tides	1.17	0.82	0.48
Harima Sea	original	1.15	0.91	0.39
	+ wave breaking	0.98	0.90	0.32
	+ tides	1.15	0.91	0.39
	+ wave breaking and tides	0.99	0.90	0.32
Ariake Sea	original	1.44	0.93	0.42
	+ wave breaking	1.23	0.92	0.33
	+ tides	1.42	0.94	0.40
	+ wave breaking and tides	1.20	0.93	0.31

Table 7 Correlation between Estimated Wave Period and Observed Wave Period

Sea	Model	Regression coefficient	Correlation coefficient	Root mean square of error (s)
Ise Bay	original	1.17	0.61	1.6
	+ wave breaking	1.17	0.62	1.5
	+ tides	1.20	0.61	1.7
	+ wave breaking and tides	1.20	0.61	1.6
Harima Sea	original	0.98	0.71	1.3
	+ wave breaking	0.97	0.71	1.3
	+ tides	1.01	0.69	1.3
	+ wave breaking and tides	1.00	0.69	1.3
Ariake Sea	original	0.91	0.55	1.3
	+ wave breaking	0.89	0.53	1.2
	+ tides	0.91	0.55	1.3
	+ wave breaking and tides	0.89	0.53	1.2

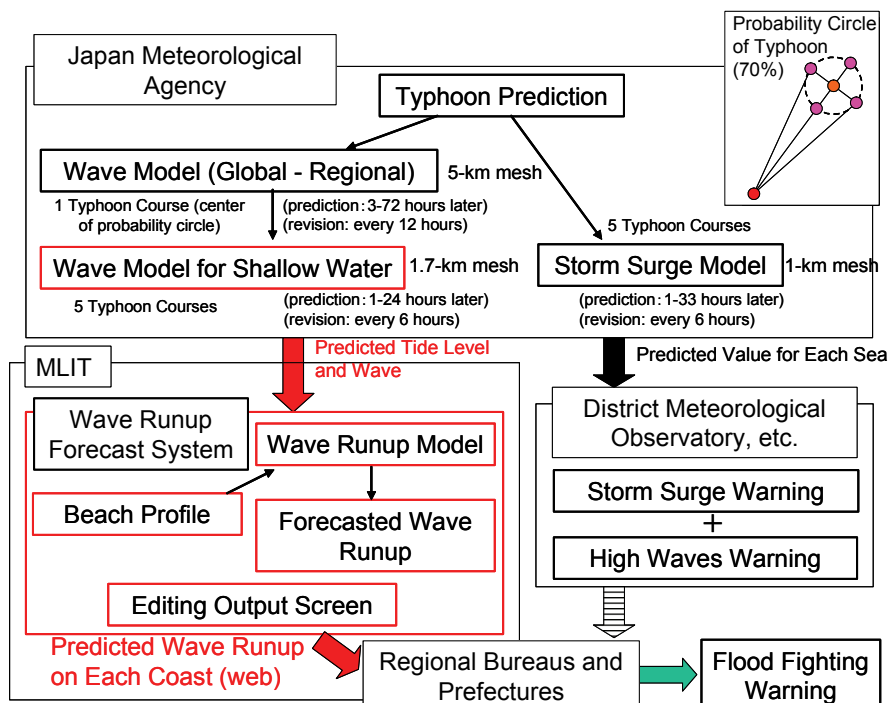


Fig.1 Constitution of the System

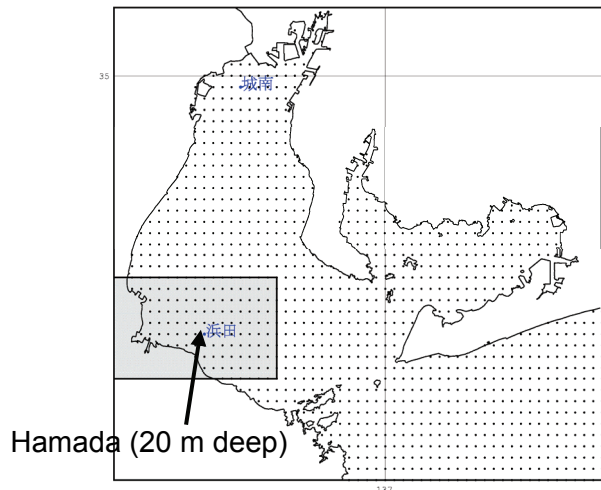


Fig. 2 Middle Area and Narrow Area (Grayed) in Ise Bay (Arrow: Wave Observatory)

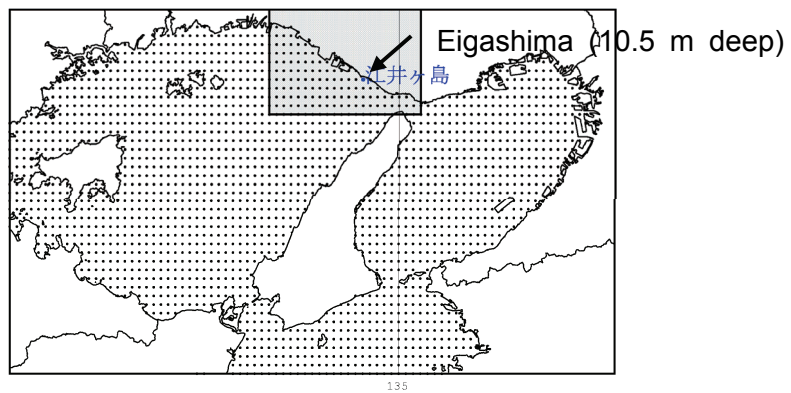


Fig. 3 Middle Area and Narrow Area (Grayed) in Harima Sea (Arrow: Wave Observatory)

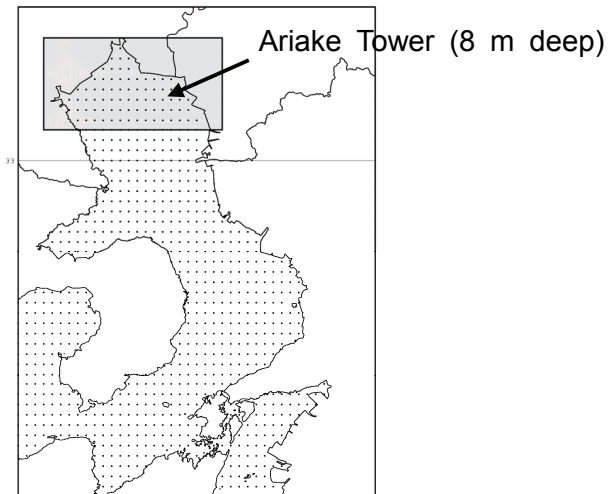


Fig. 4 Middle Area and Narrow Area (Grayed) in Ariake Sea (Arrow: Wave Observatory)

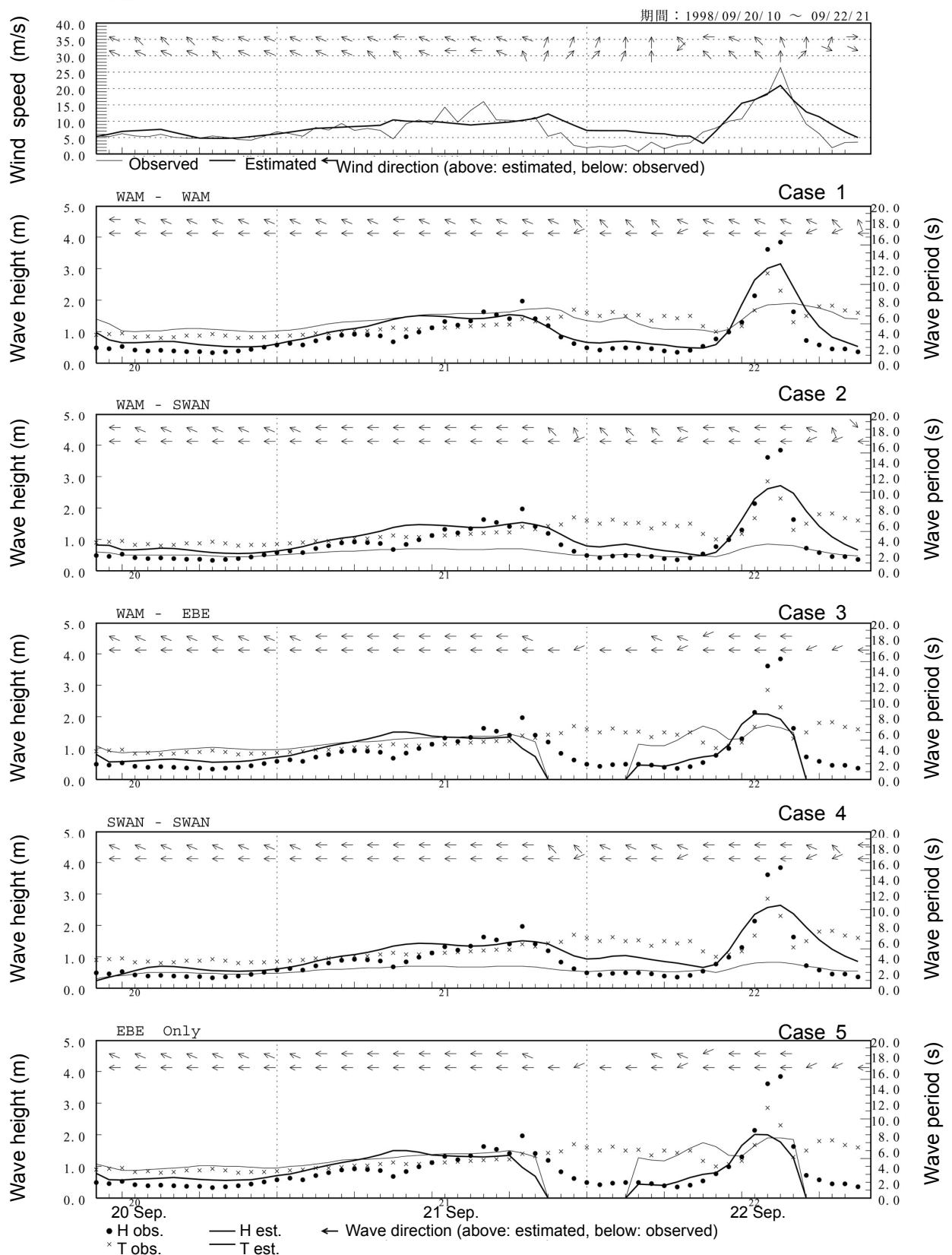


Fig. 5 Time Series of Winds and Waves in Typhoon 9807

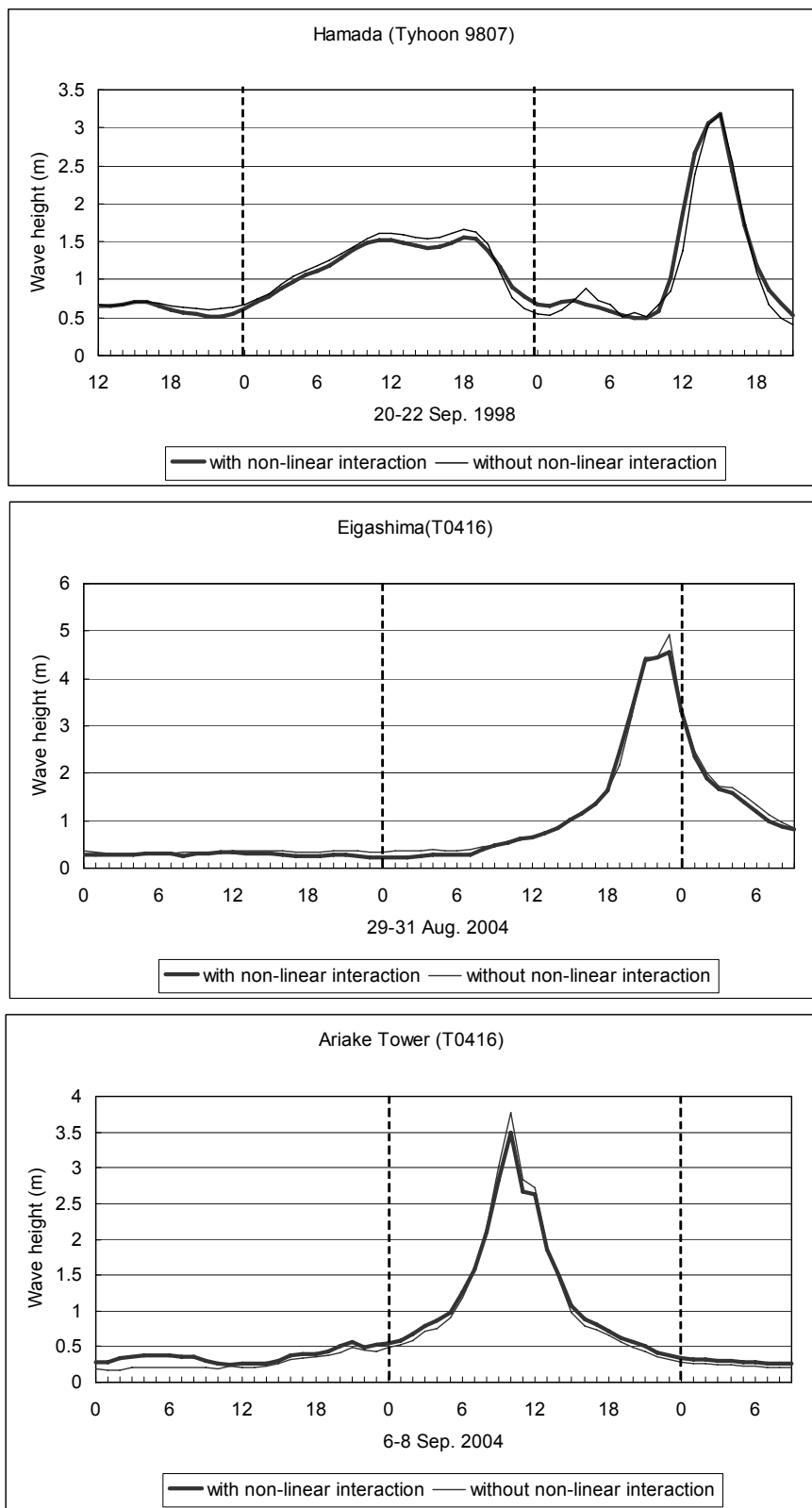


Fig. 6 Effects of Nonlinear Wave-Wave Interaction (upper: Hamada; middle: Eigashima; lower: Ariake Tower)

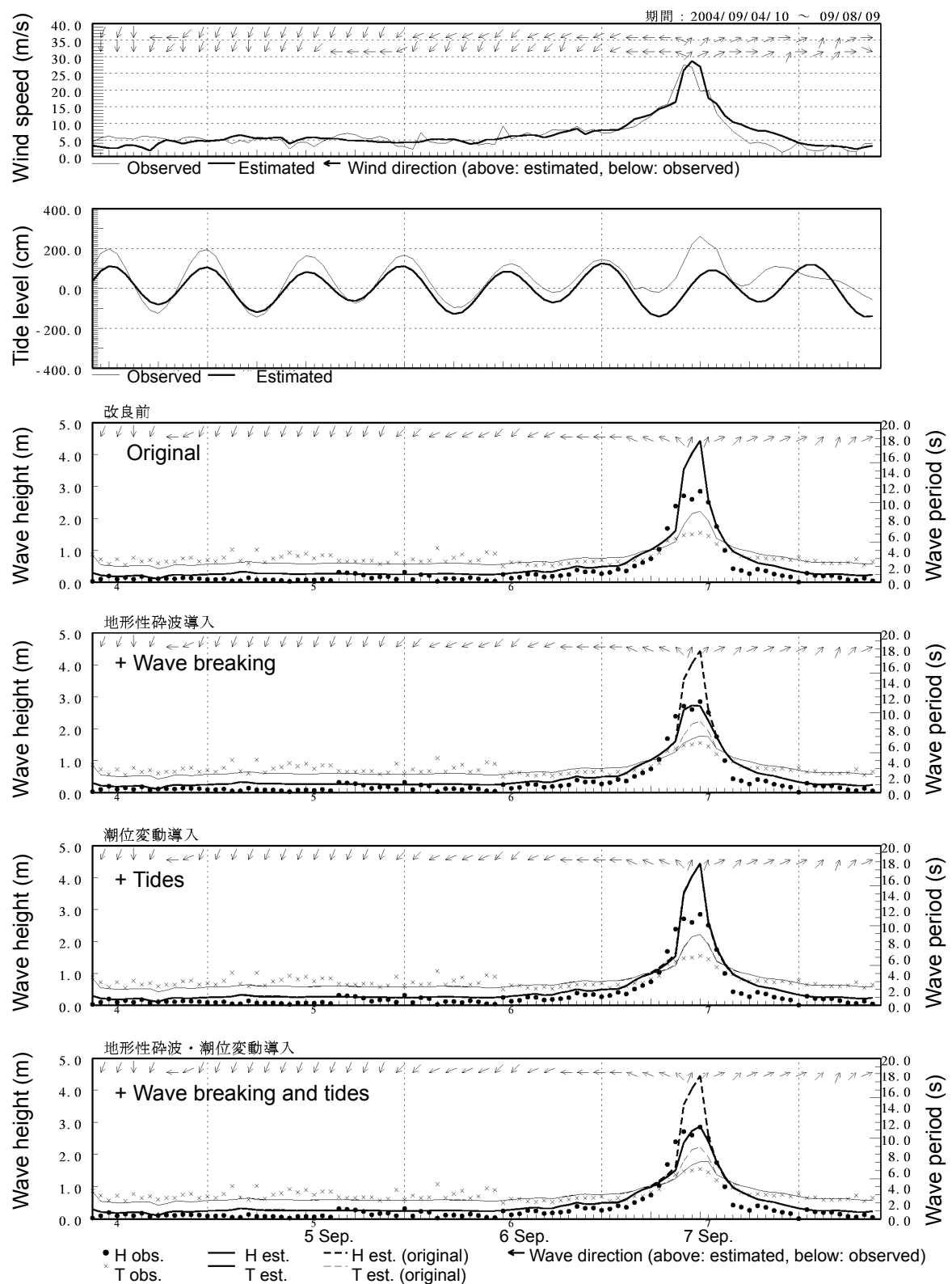


Fig. 7 Comparison between Estimation and Observation (Typhoon 0418, Ariake Tower)